EUROPEAN ORGANIZATION FOR NUCLEAR RESEARCH

CERN–PPE/93–30
February 18, 1993

A Search for the Neutral Higgs Boson at LEP

L3 Collaboration

Abstract

We update the results of a search for the Standard Model neutral Higgs boson using a data sample corresponding to 1,062,000 hadronic Z decays. We exclude the existence of the Minimal Standard Model Higgs boson in the mass range $0 \leq m_{\mathrm{H}} < 57.7$ GeV at the 95% confidence level.

(Submitted to *Physics Letters B*)

1 Introduction

The Minimal Standard Model [1] predicts the existence of a neutral scalar Higgs particle H^0 [2]. In the framework of this model the couplings of the H^0 boson to the fermions and to the gauge vector bosons are known but its mass is not specified.

The main production mechanism of the Higgs boson at LEP is predicted to be through the decay of the Z boson into an H^0 and a virtual Z^* [3]

$$e^+e^- \to Z \to H^0 + Z^* \to H^0 + f\bar{f}.$$

A heavy Higgs boson (with mass exceeding 11 GeV) decays predominantly into a $b\bar{b}$ pair, although the branching ratios into $c\bar{c}$ and $\tau^+\tau^-$ are not negligible [4]. With QCD corrections [5] the branching ratio into $\tau^+\tau^-$ for a 60 GeV Higgs boson is approximately 5.7%.

We have previously reported on searches for the Standard Model Higgs boson using the 1990 and 1991 data sample, corresponding to 17.5 pb^{-1} integrated luminosity around the Z pole [6, 7]. These searches allowed us to exclude the presence of the Higgs boson in the mass range $0 \leq m_H < 52.0$ GeV at the 95% confidence level. Searches have also been performed by the other LEP experiments [8, 9, 10].

Using the same analysis method we have expanded the search for the H^0 by including our 1992 data sample, corresponding to 654,000 Z hadronic decays. Altogether this totals 1,062,000 hadronic Z decays and 39.0 pb^{-1} integrated luminosity at center of mass energies between 88.2 and 94.3 GeV.

We report here on updated results of the search for the Higgs boson in the mass range from 30 to 70 GeV. We have searched in the channels $H^0\nu\bar{\nu}$, $H^0e^+e^-$, $H^0\mu^+\mu^-$, where the signal has the most distinctive signatures.

2 The L3 Detector

The L3 detector consists of a central tracking chamber, a high resolution electromagnetic calorimeter composed of BGO crystals, a ring of scintillation counters, a uranium and brass hadron calorimeter with proportional wire chamber readout, and an accurate muon chamber system. These detectors are installed in a 12 m diameter magnet which provides a uniform field of 0.5 T along the beam direction. For hadronic jets the fiducial coverage is 99% of 4π.

We have previously presented the detector and its performance in detail [11, 12]. Here we briefly describe the subdetectors relevant for this analysis.

The central tracking chamber (TEC) is a time expansion chamber which consists of two cylindrical layers of 12 (inner) and 24 (outer) sectors, with 62 wires measuring the r–ϕ coordinate. The single wire resolution is 58 μm averaged over the entire cell. The double-track resolution is 640 μm. The BGO electromagnetic calorimeter, which includes endcaps installed in 1991, covers 85% of the solid angle. The fine segmentation of the BGO detector and hadron calorimeter allows us to measure the direction of jets with an angular resolution of 2.1°, and to measure the total energy of hadronic events from Z decays with a resolution of 10.2%. The muon detector consists of 3 layers of precise drift chambers, which measure 56 points on the muon trajectory in the bending plane, and 8 points in the non-bending direction.

The response of the detector was simulated using the L3 detector simulation program [13, 14] which takes into account the effects of energy loss, multiple scattering, interactions and decays and includes the detector efficiency and resolution.

As the selections described below extensively use the information coming from the calorimetric part of the detector, we briefly describe the related reconstruction algorithm. Jets are reconstructed using a two step procedure [12]: firstly neighbouring calorimetric hits are combined into clusters, then jets are formed merging neighbouring clusters and muon tracks. Each charged track measured in the tracking chamber is assigned to the nearest jet. The algorithm normally reconstructs one such 'jet' for a single isolated electron, photon, muon, high energy τ or a hadronic jet. Unless otherwise stated in the following jets are defined by this algorithm.

3 $\mathrm{H}^0\nu\bar{\nu}$ Event Selection

$\mathrm{H}^0\nu\bar{\nu}$ events are characterized by large missing energy and momentum imbalance due to the undetected neutrinos from the Z^* decay. The heavy quarks from the Higgs decay receive a Lorentz boost leading to two acoplanar jets which mainly populate one hemisphere with a rather low energy deposit in the other. The direction of the missing energy, being mainly that of the Z^*, is far from the quark jets. In contrast, in $\mathrm{e}^+\mathrm{e}^- \rightarrow \mathrm{q}\bar{\mathrm{q}}$ events (the main background), the two jets from the $\mathrm{q}\bar{\mathrm{q}}$ system are typically coplanar with the beam axis, seldom leading to low energy deposits in any one hemisphere. The relatively small missing energy is mostly due to the jet energy resolution or the undetected neutrinos within the jets. As a consequence the missing energy direction is close to one of the jet axes.

The search for Higgs candidates is carried out taking advantage of these signatures.

In the preselection a set of cuts is applied to eliminate a large fraction of the background due to the $\mathrm{q}\bar{\mathrm{q}}$, $\tau^+\tau^-$, two photon processes, cosmic rays and beam gas interactions. We require that:

- The invariant mass of the event calculated from all the calorimetric clusters (assumed to be massless), M_{vis}, is within the range 25–70 GeV.

- The energy imbalance transverse to the beam axis is larger than 15% and that parallel to the beam axis is less than 45% of the visible energy. The direction of the energy imbalance is more than 0.4 rad away from the beam axis.

- There are more than 4 charged tracks with transverse momenta larger than 0.3 GeV and with distances of closest approach to the beam axis less than 5 mm and there are more than 15 calorimetric clusters.

The acceptance of the above cuts including trigger efficiency for $\mathrm{H}^0\nu\bar{\nu}$ events with m_{H} of 60 GeV is 73% and we are left with 1.2% of the hadronic Z decays, the background from all other sources being negligible.

For the final selection we use a set of cuts based on topological variables which are mostly related to the jet axis measurement since the jet directions are usually well defined even for events with large missing energy. The jet reconstruction starts by identifying the two calorimetric clusters that have the largest invariant mass. The plane perpendicular to that containing the direction vectors of the two clusters and bisecting the angle defined by them divides the event into two hemispheres. All the clusters in each hemisphere are combined to form a jet whose direction is determined by adding the momentum vectors of the clusters. Hence we obtain exactly two jets for each event, corresponding to the primary $\mathrm{q}\bar{\mathrm{q}}$ pair. The energies of both reconstructed jets are required to exceed 8 GeV. We define then a unit vector $\hat{b}$ which is opposite to the sum of the unit vectors along the two jet directions.

Finally, we use the set of cuts from our previous publication [7]. An event is accepted if it satisfies the following criteria:

- $E_{90} < 10$ GeV and $E_{60} < 3$ GeV, where E_{90} and E_{60} are the energies deposited in the cones with half opening angles of 90° and 60° respectively around $\hat{b}$.
- The largest angular region, in the r–ϕ plane, where no tracks are present must be greater than 1.1 rad.
- $E_I < 1$ GeV, where E_I is the energy deposited in a cone of 20° half opening angle around the missing energy direction.
- $\xi < 160°$ and $\zeta < 170°$, where ξ and ζ are the angles between the two jets in space and in the r–ϕ plane respectively.

The above selection is sensitive only to the decays of the Higgs boson into $\mathrm{q\bar{q}}$ pairs. In order to improve the selection efficiency by detecting decays $\mathrm{H^0} \rightarrow \tau^+\tau^-$ we alternatively use the following selection criteria:

- There are less than 18 calorimetric clusters and the total energy of all the calorimetric clusters is within the range 15–75 GeV.
- The energy imbalance transverse to the beam axis is larger than 5 GeV and that parallel to the beam axis is less than 45% of the visible energy.
- There are 2 charged narrow jets. We define narrow jets as those which have the ratio of calorimetrical energies in 15° and 30° cones around their axes exceeding 0.9.
- $E_{90} < 3$ GeV and $E_{60} < 1.5$ GeV.
- The largest angular region in the r–ϕ plane where no tracks are present is greater than 3.0 rad.
- the angle between the two jets in the r–ϕ plane is less than 160°.

The overall detection efficiency for the Higgs signal as a function of the $\mathrm{H^0}$ mass is shown in Table 1.

The relative uncertainty in the selection efficiency has been found to be less than 1.5% for a 60 GeV Higgs mass [7].

No candidates have been found in our data sample, and no events pass the selection from a sample of 1,140,000 $\mathrm{q\bar{q}}$ Monte Carlo [14] events.

4 $\mathrm{H^0e^+e^-}$ Event Selection

The signature of this process is the presence of two energetic and well separated electrons coming from the virtual $\mathrm{Z^*}$ isolated from the $\mathrm{H^0}$ decay products. The main sources of background are the four fermion process $\mathrm{e^+e^-} \rightarrow \mathrm{e^+e^-q\bar{q}}$ [15] and the double semileptonic decay $\mathrm{Z} \rightarrow \mathrm{b\bar{b}} \rightarrow \mathrm{e^+e^-}X$.

In our selection low multiplicity events, such as $\mathrm{e^+e^-}$ and $\tau^+\tau^-$ final states, are removed by requiring at least 15 clusters in the electromagnetic calorimeter.

To reduce the hadronic background in our sample we require that the two most energetic clusters have energies greater than 3 GeV and that the sum of their energies exceeds 15 GeV; in addition the opening angle between these two clusters must be larger than 40°.

The identification of electromagnetic particles is mainly based on the energy deposition pattern in the electromagnetic calorimeter. We consider the ratio of the energy deposited in a 3×3 crystal array and the energy deposited in a 5×5 array both centred on the most energetic crystal in the cluster. After applying a position-dependent leakage correction to both measurements the distribution of this ratio is approximately gaussian, centered at 1.0 with a width of 1%. Electromagnetic candidates are identified by requiring that this ratio is less than 3σ away from the above mean value.

The isolation of the electron candidates is further ensured by imposing the following conditions:

- The additional energy deposited in the electromagnetic calorimeter in a cone of 15° half opening angle around the direction of the highest energy cluster must not exceed 5% of the cluster energy and the energy measured in the hadron calorimeter in the same cone must be less than 3 GeV.

- The additional energy deposited in the electromagnetic calorimeter in a cone of 15° half opening angle around the second most energetic cluster must not exceed 7% of its energy.

To complete the identification of the electrons we consider all pairs out of three most energetic electron candidates. The most energetic cluster in the pair is required to match in azimuthal angle with exactly one track and the second most energetic cluster with at least one track. For both clusters the matching has to be within a 4 σ cut where σ depends on the energies and on the polar angles of the clusters.

To identify the Higgs boson decay products we examine the non-electron jets in the event. Indicating with $P_\perp$ the transverse momentum of each electron with respect to the nearest jet, we require the sum of the two $P_\perp$ to be larger than 10 GeV.

To reject a background from the four fermion process we require that:

$$2M_{\mathrm{e^+e^-}} + M_{miss} > 80 \text{ GeV}$$

where $M_{\mathrm{e^+e^-}}$ is the invariant mass of the electron pair and M_{miss} is the missing mass with respect to these electrons. Figure 1 shows the effect of this cut on the remaining candidates as well as on the expected Higgs signal after all above cuts are applied.

The selection efficiencies for the signal are shown in Table 1 for the 1990 and 1991–1992 setups. The efficiency for the 1990 data is lower due to the lower geometrical acceptance of the BGO calorimeter which did not include the endcaps.

Two events passed the above selection criteria. The first one, with the missing mass to two electrons of 31.4 ± 1.5 GeV, is from the 1991 data sample [7]; the second one, from the 1992 data sample, has the missing mass recoiling against the electron pair of 67.6 ± 0.7 GeV. This event is shown in Figure 2 and its main parameters are given in Table 2. Both events are consistent with the background process $\mathrm{e^+e^-} \rightarrow \mathrm{e^+e^-q\bar{q}}$ from which we expect 2.5 ± 0.4 events. The background from other processes is negligible.

5 $\mathrm{H}^0\mu^+\mu^-$ Event Selection

This analysis is based on the selection of events with well isolated muons together with other charged particles present in the fragmentation of the heavy quark pair from the Higgs decay.

Muons are identified as tracks in the muon spectrometer that when extrapolated back towards the beam line pass within 3.5σ from the interaction point, both in the r–ϕ and z directions; in the following we refer to these tracks simply as muons.

We require the presence of at least one muon and at least 5 other tracks reconstructed in the TEC in order to remove cosmic ray, $\mu^+\mu^-$, $\tau^+\tau^-$, $\mathrm{e^+e^-}\mu^+\mu^-$ and $\pi^+\pi^+\mu^+\mu^-$ events. In order to reduce the background from $\mathrm{Z} \rightarrow \mathrm{q\bar{q}}$ events, we require the event thrust to be less than 0.92.

To further reduce the background from the semileptonic decays of hadrons two sets of cuts are applied: set *(i)* to recognize a single well isolated muon and set *(ii)* to select the muon pair from the Z^* decay. An event is accepted as a candidate if it has at least one muon satisfying the first set of cuts *(i)* or at least a pair of muons satisfying the second set of cuts *(ii)*. This allows us to recover the events in which one of the two muons coming from the decay of the virtual Z^* is not detected in the muon spectrometer.

To measure the isolation of a muon we define three quantities.

- $\mathcal{D}_i = \frac{E_{jet_i} - p_{\mu_i}}{p_{\mu_i}}$, where E_{jet_i} is the energy of the jet which includes the i^{th} muon and p_{μ_i} is the value of the muon momentum.

- $\mathcal{E}_i^e$ and $\mathcal{E}_i^h$ are the differences of the energies deposited in 30° and 3° cones around the i^{th} muon in the BGO and hadron calorimeters respectively. The subtraction diminishes the sensitivity of this variable to radiative photons.

The two sets of cuts are:

Set (i)

The muon must have a momentum larger than 10 GeV. To ensure the isolation, we require less than 5 calorimetric clusters and at most one additional charged track, which must be isolated by more than 0.1 rad, in the jet which includes the muon. The isolation variable $\mathcal{D}$ must have a value of less than 0.3, and the variable $\mathcal{E}^e$ must be less than 2 GeV. In addition the missing energy of the event is required to be at least 10 GeV due to the undetected muon.

Set (ii)

The opposite-sign muon pair is identified as being from the decay of the Z^* if it satisfies the following criteria:

- There is at least one muon with less than 5 charged tracks in the associated jet.

- $\mathcal{D}_1 \cdot \mathcal{D}_2 < 0.7$.

- $\min(\mathcal{E}_1^e, \mathcal{E}_2^e) < 250$ MeV.

- $\min(\mathcal{E}_1^h, \mathcal{E}_2^h) < 1$ GeV.

- $\min(p_{\mu_1}, p_{\mu_2}) > 3.4$ GeV and $p_{\mu_1} + p_{\mu_2} > 15$ GeV.

In order to suppress the background from four fermion processes we use the same final cut as in the $\mathrm{H^0e^+e^-}$ selection:

$$2M_{\mu^+\mu^-} + M_{miss} > 80 \text{ GeV}$$

For events passing selection *(i)* we compute $M_{\mu^+\mu^-}$ and M_{miss} in the following way: if there is a TEC track pointing to a calorimetric cluster compatible with a minimum ionizing particle, the undetected muon momentum vector is assumed to be the one measured by the TEC; if there is no such track, the undetected muon momentum vector is assumed to be the missing momentum vector of the event.

The Higgs selection efficiencies are shown in Table 1.

One event with $M_{miss} = 70.4 \pm 0.7$ GeV from the 1991 data sample passed the above selection criteria [7]. The expected background is computed to be 1.2 ± 0.2 events.

6 Systematic Uncertainties

The sources of systematic errors on the number of expected Higgs events are the following:

- Theoretical uncertainty of less than 1% on the ratio between the Higgs boson production cross section and the $e^+e^- \rightarrow q\bar{q}$ cross section [16].
- Experimental uncertainty of 0.5% on the corrected number of hadronic Z decays used for the normalization.
- Theoretical uncertainty on the Higgs decay branching ratios which contributes an error of 0.7% to the detection efficiency [5].
- Error on the Higgs detection efficiency of 1.5% due to the uncertainties in the fragmentation model and due to the uncertainties in the detector calibration constants [7].
- Error on the Higgs detection efficiency of 1.5% due to Monte Carlo statistics.

Combining these errors in quadrature we obtain a systematic uncertainty of 2.5%.

7 Mass Limit

We have observed two e^+e^- hadrons and one $\mu^+\mu^-$ hadrons events that pass our selection criteria. From Monte Carlo studies, we expect the number of background events to be 2.5 ± 0.4 $e^+e^-q\bar{q}$ for the $H^0e^+e^-$channel and 1.2 ± 0.2 $\mu^+\mu^-q\bar{q}$ for the $H^0\mu^+\mu^-$ channel. Taking into account the mass resolution of the L3 detector we conclude that none of these events is consistent with a Higgs boson mass in the vicinity of 60 GeV. Therefore we take the 95% confidence level limit on the Higgs boson mass corresponding to 3 events. Taking into account the 2.5% systematic error on the number of expected events, we obtain a 95% C.L. lower limit on the mass of the Higgs boson of 57.7 GeV.

Figure 3 shows the number of expected Higgs events in the mass range from 30 to 70 GeV. The 95% C.L. line, also shown in the figure, was obtained with the likelihood function of the candidates, taking into account the number of expected events from the background and the mass measurement errors.

Acknowledgments

We wish to express our gratitude to the CERN accelerator divisions for the excellent performance of the LEP machine. We acknowledge the efforts of all engineers and technicians who have participated in the construction and maintenance of this experiment.

The L3 Collaboration:

O.Adriani,[14] M.Aguilar-Benitez,[23] S.Ahlen,[9] J.Alcaraz,[15] A.Aloisio,[26] G.Alverson,[10] M.G.Alviggi,[26] G.Ambrosi,[31] Q.An,[16] H.Anderhub,[45] A.L.Anderson,[13] V.P.Andreev,[35] L.Antonov,[39] D.Antreasyan,[7] P.Arce,[23] A.Arefiev,[25] A.Atamanchuk,[35] T.Azemoon,[3] T.Aziz,[1,8] P.V.K.S.Baba,[16] P.Bagnaia,[34] J.A.Bakken,[33] L.Baksay,[41] R.C.Ball,[3] S.Banerjee,[8] J.Bao,[5] R.Barillère,[15] L.Barone,[34] A.Baschirotto,[24] R.Battiston,[31] A.Bay,[17] F.Becattini,[14] U.Becker,[13,45] F.Behner,[45] J.Behrens,[45] Gy.L.Bencze,[11] J.Berdugo,[23] P.Berges,[13] B.Bertucci,[31] B.L.Betev,[39,45] M.Biasini,[31] A.Biland,[45] G.M.Bilei,[31] R.Bizzarri,[34] J.J.Blaising,[4] G.J.Bobbink,[15,2] R.Bock,[1] A.Böhm,[1] B.Borgia,[34] M.Bosetti,[24] D.Bourilkov,[28] M.Bourquin,[17] D.Boutigny,[4] B.Bouwens,[2] E.Brambilla,[26] J.G.Branson,[36] I.C.Brock,[32] M.Brooks,[21] A.Bujak,[42] J.D.Burger,[13] W.J.Burger,[17] J.Busenitz,[41] A.Buytenhuijs,[28] X.D.Cai,[16] M.Capell,[20] M.Caria,[31] G.Carlino,[26] A.M.Cartacci,[14] R.Castello,[24] M.Cerrada,[23] F.Cesaroni,[34] Y.H.Chang,[13] U.K.Chaturvedi,[16] M.Chemarin,[22] A.Chen,[47] C.Chen,[6] G.M.Chen,[6] H.F.Chen,[18] H.S.Chen,[6] M.Chen,[13] W.Y.Chen,[47] G.Chiefari,[26] C.Y.Chien,[5] M.T.Choi,[40] S.Chung,[13] C.Civinini,[14] I.Clare,[13] R.Clare,[13] T.E.Coan,[21] H.O.Cohn,[29] G.Coignet,[4] N.Colino,[15] A.Contin,[7] X.T.Cui,[16] X.Y.Cui,[16] T.S.Dai,[13] R.D'Alessandro,[14] R.de Asmundis,[26] A.Degré,[4] K.Deiters,[43] E.Dénes,[11] P.Denes,[33] F.DeNotaristefani,[34] M.Dhina,[45] D.DiBitonto,[41] M.Diemoz,[34] H.R.Dimitrov,[39] C.Dionisi,[34,15] L.Djambazov,[45] M.T.Dova,[16] E.Drago,[26] D.Duchesneau,[17] P.Duinker,[2] I.Duran,[37] S.Easo,[31] H.El Mamouni,[22] A.Engler,[32] F.J.Eppling,[13] F.C.Erné,[2] P.Extermann,[17] R.Fabbretti,[43] M.Fabre,[43] S.Falciano,[34] S.J.Fan,[38] O.Fackler,[20] J.Fay,[22] M.Felcini,[15] T.Ferguson,[32] D.Fernandez,[23] G.Fernandez,[23] F.Ferroni,[34] H.Fesefeldt,[1] E.Fiandrini,[31] J.Field,[17] F.Filthaut,[28] G.Finocchiaro,[34] P.H.Fisher,[5] G.Forconi,[17] T.Foreman,[2] K.Freudenreich,[45] W.Friebel,[44] M.Fukushima,[13] M.Gailloud,[19] Yu.Galaktionov,[25,13] E.Gallo,[14] S.N.Ganguli,[15,8] P.Garcia-Abia,[23] D.Gele,[22] S.Gentile,[34,15] S.Goldfarb,[10] Z.F.Gong,[18] E.Gonzalez,[23] A.Gougas,[5] D.Goujon,[17] G.Gratta,[30] M.Gruenewald,[30] C.Gu,[16] M.Guanziroli,[16] J.K.Guo,[38] V.K.Gupta,[33] A.Gurtu,[8] H.R.Gustafson,[3] L.J.Gutay,[42] K.Hangarter,[1] B.Hartmann,[1] A.Hasan,[16] D.Hauschildt,[2] C.F.He,[38] J.T.He,[6] T.Hebbeker,[1] M.Hebert,[36] G.Herten,[13] A.Hervé,[15] K.Hilgers,[1] H.Hofer,[45] H.Hoorani,[17] G.Hu,[16] G.Q.Hu,[38] B.Ille,[22] M.M.Ilyas,[16] V.Innocente,[15] H.Janssen,[15] S. Jezequel,[4] B.N.Jin,[6] L.W.Jones,[3] A.Kasser,[19] R.A.Khan,[16] Yu.Kamyshkov,[29] P.Kapinos,[35,44] J.S.Kapustinsky,[21] Y.Karyotakis,[15] M.Kaur,[16] S.Khokhar,[16] M.N.Kienzle-Focacci,[17] J.K.Kim,[40] S.C.Kim,[40] Y.G.Kim,[40] W.W.Kinnison,[21] D.Kirkby,[30] S.Kirsch,[44] W.Kittel,[28] A.Klimentov,[13,25] A.C.König,[28] E.Koffeman,[2] O.Kornadt,[1] V.Koutsenko,[13,25] A.Koulbardis,[35] R.W.Kraemer,[32] T.Kramer,[13] V.R.Krastev,[39,31] W.Krenz,[1] A.Krivshich,[35] H.Kuijten,[28] K.S.Kumar,[12] A.Kunin,[12,25] G.Landi,[14] D.Lanske,[1] S.Lanzano,[26] P.Lebrun,[22] P.Lecomte,[45] P.Lecoq,[15] P.Le Coultre,[45] D.M.Lee,[21] I.Leedom,[10] C.Leggett,[3] J.M.Le Goff,[15] R.Leiste,[44] M.Lenti,[14] E.Leonardi,[34] X.Leytens,[2] C.Li,[18,16] H.T.Li,[6] P.J.Li,[38] J.Y.Liao,[38] W.T.Lin,[47] Z.Y.Lin,[18] F.L.Linde,[15] B.Lindemann,[1] L.Lista,[26] Y.Liu,[16] W.Lohmann,[44,15] E.Longo,[34] Y.S.Lu,[6] J.M.Lubbers,[15] K.Lübelsmeyer,[1] C.Luci,[34] D.Luckey,[7,13] L.Ludovici,[34] L.Luminari,[34] W.Lustermann,[44] J.M.Ma,[6] W.G.Ma,[18] M.MacDermott,[45] P.K.Malhotra,[8,†] R.Malik,[16] A.Malinin,[25] C.Maña,[23] M.Maolinbay,[45] P.Marchesini,[45] F.Marion,[4] A.Marin,[9] J.P.Martin,[22] L.Martinez-Laso,[23] F.Marzano,[34] G.G.G.Massaro,[2] K.Mazumdar,[8] P.McBride,[12] T.McMahon,[42] D.McNally,[45] M.Merk,[32] L.Merola,[26] M.Meschini,[14] W.J.Metzger,[28] Y.Mi,[19] G.B.Mills,[21] Y.Mir,[16] G.Mirabelli,[34] J.Mnich,[1] M.Möller,[1] B.Monteleoni,[14] R.Morand,[4] S.Morganti,[34] N.E.Moulai,[16] R.Mount,[30] S.Müller,[1] A.Nadtochy,[35] E.Nagy,[11] M.Napolitano,[26] F.Nessi-Tedaldi,[45] H.Newman,[30] C.Neyer,[45] M.A.Niaz,[16] A.Nippe,[1] H.Nowak,[44] G.Organtini,[34] D.Pandoulas,[1] S.Paoletti,[14] P.Paolucci,[26] G.Pascala,[34] G.Passaleva,[14,31] S.Patricelli,[26] T.Paul,[5] M.Pauluzzi,[31] C.Paus,[1] F.Pauss,[45] Y.J.Pei,[1] S.Pensotti,[24] D.Perret-Gallix,[4] J.Perrier,[17] A.Pevsner,[5] D.Piccolo,[26] M.Pieri,[15] P.A.Piroué,[33] F.Plasil,[29] V.Plyaskin,[25] M.Pohl,[45] V.Pojidaev,[25,14] H.Postema,[13] Z.D.Qi,[38] J.M.Qian,[3] K.N.Qureshi,[16] R.Raghavan,[8] G.Rahal-Callot,[45] P.G.Rancoita,[24] M.Rattaggi,[24] G.Raven,[2] P.Razis,[27] K.Read,[29] D.Ren,[45] Z.Ren,[16] M.Rescigno,[34] S.Reucroft,[10] A.Ricker,[1] S.Riemann,[44] B.C.Riemers,[42] K.Riles,[3] O.Rind,[3] H.A.Rizvi,[16] F.J.Rodriguez,[23] B.P.Roe,[3] M.Röhner,[1] S.Röhner,[1] L.Romero,[23] J.Rose,[1] S.Rosier-Lees,[4] R.Rosmalen,[28] Ph.Rosselet,[19] W.van Rossum,[2] S.Roth,[1] A.Rubbia,[13] J.A.Rubio,[15] H.Rykaczewski,[45] M.Sachwitz,[44] J.Salicio,[15] J.M.Salicio,[23] G.S.Sanders,[21] A.Santocchia,[31] M.S.Sarakinos,[13] G.Sartorelli,[7,16] M.Sassowsky,[1] G.Sauvage,[4] V.Schegelsky,[35] D.Schmitz,[1] P.Schmitz,[1] M.Schneegans,[4] H.Schopper,[46] D.J.Schotanus,[28] S.Shotkin,[13] H.J.Schreiber,[44] J.Shukla,[32] R.Schulte,[1] S.Schulte,[1] K.Schultze,[1] J.Schwenke,[1] G.Schwering,[1] C.Sciacca,[26] I.Scott,[12] R.Sehgal,[16] P.G.Seiler,[43] J.C.Sens,[15,2] L.Servoli,[31] I.Sheer,[36] D.Z.Shen,[38] S.Shevchenko,[30] X.R.Shi,[30] E.Shumilov,[25] V.Shoutko,[25] D.Son,[40] A.Sopczak,[36] C.Spartiotis,[5] T.Spickermann,[1] P.Spillantini,[14] R.Starosta,[1] M.Steuer,[7,13] D.P.Stickland,[33] F.Sticozzi,[13] H.Stone,[33] K.Strauch,[12] B.C.Stringfellow,[42] K.Sudhakar,[8] G.Sultanov,[16] L.Z.Sun,[18,16] H.Suter,[45] J.D.Swain,[16] O.Syben,[1] A.A.Syed,[28] X.W.Tang,[6] L.Taylor,[10] G.Terzi,[24] Samuel C.C.Ting,[13] S.M.Ting,[13] M.Tonutti,[1] S.C.Tonwar,[8] J.Tóth,[11] A.Tsaregorodtsev,[35] G.Tsipolitis,[32] C.Tully,[33] K.L.Tung,[6] J.Ulbricht,[45] L.Urbán,[11] U.Uwer,[1] E.Valente,[34] R.T.Van de Walle,[28] I.Vetlitsky,[25] G.Viertel,[45] P.Vikas,[16] U.Vikas,[16] M.Vivargent,[4] H.Vogel,[32] H.Vogt,[44] I.Vorobiev,[25] A.A.Vorobyov,[35] L.Vuilleumier,[19] M.Wadhwa,[4] W.Wallraff,[1] C.Wang,[13] C.R.Wang,[18] G.H.Wang,[32] X.L.Wang,[18] Y.F.Wang,[13] Z.M.Wang,[16,18] A.Weber,[1] J.Weber,[45] R.Weill,[19] T.J.Wenaus,[20] J.Wenninger,[17] M.White,[13] C.Willmott,[23] F.Wittgenstein,[15] D.Wright,[33] S.X.Wu,[16] B.Wysłouch,[13] Y.Y.Xie,[38] J.G.Xu,[6] Z.Z.Xu,[18] Z.L.Xue,[38] D.S.Yan,[38] B.Z.Yang,[18] C.G.Yang,[6] G.Yang,[16] C.H.Ye,[16] J.B.Ye,[18] Q.Ye,[16] S.C.Yeh,[47] Z.W.Yin,[38] J.M.You,[16] N.Yunus,[16] M.Yzerman,[2] C.Zaccardelli,[30] P.Zemp,[45] M.Zeng,[16] Y.Zeng,[1] D.H.Zhang,[2] Z.P.Zhang,[18,16] B.Zhou,[9] G.J.Zhou,[6] J.F.Zhou,[1] R.Y.Zhu,[30] A.Zichichi,[7,15,16] B.C.C.van der Zwaan.[2]

1 I. Physikalisches Institut, RWTH, W-5100 Aachen, FRG§
III. Physikalisches Institut, RWTH, W-5100 Aachen, FRG§
2 National Institute for High Energy Physics, NIKHEF, NL-1009 DB Amsterdam, The Netherlands
3 University of Michigan, Ann Arbor, MI 48109, USA
4 Laboratoire d'Annecy-le-Vieux de Physique des Particules, LAPP,IN2P3-CNRS, BP 110, F-74941 Annecy-le-Vieux CEDEX, France
5 Johns Hopkins University, Baltimore, MD 21218, USA
6 Institute of High Energy Physics, IHEP, 100039 Beijing, China
7 INFN-Sezione di Bologna, I-40126 Bologna, Italy
8 Tata Institute of Fundamental Research, Bombay 400 005, India
9 Boston University, Boston, MA 02215, USA
10 Northeastern University, Boston, MA 02115, USA
11 Central Research Institute for Physics of the Hungarian Academy of Sciences, H-1525 Budapest 114, Hungary‡
12 Harvard University, Cambridge, MA 02139, USA
13 Massachusetts Institute of Technology, Cambridge, MA 02139, USA
14 INFN Sezione di Firenze and University of Florence, I-50125 Florence, Italy
15 European Laboratory for Particle Physics, CERN, CH-1211 Geneva 23, Switzerland
16 World Laboratory, FBLJA Project, CH-1211 Geneva 23, Switzerland
17 University of Geneva, CH-1211 Geneva 4, Switzerland
18 Chinese University of Science and Technology, USTC, Hefei, Anhui 230 029, China
19 University of Lausanne, CH-1015 Lausanne, Switzerland
20 Lawrence Livermore National Laboratory, Livermore, CA 94550, USA
21 Los Alamos National Laboratory, Los Alamos, NM 87544, USA
22 Institut de Physique Nucléaire de Lyon, IN2P3-CNRS,Université Claude Bernard, F-69622 Villeurbanne Cedex, France
23 Centro de Investigaciones Energeticas, Medioambientales y Tecnologicas, CIEMAT, E-28040 Madrid, Spain
24 INFN-Sezione di Milano, I-20133 Milan, Italy
25 Institute of Theoretical and Experimental Physics, ITEP, Moscow, Russia
26 INFN-Sezione di Napoli and University of Naples, I-80125 Naples, Italy
27 Department of Natural Sciences, University of Cyprus, Nicosia, Cyprus
28 University of Nymegen and NIKHEF, NL-6525 ED Nymegen, The Netherlands
29 Oak Ridge National Laboratory, Oak Ridge, TN 37831, USA
30 California Institute of Technology, Pasadena, CA 91125, USA
31 INFN-Sezione di Perugia and Universitá Degli Studi di Perugia, I-06100 Perugia, Italy
32 Carnegie Mellon University, Pittsburgh, PA 15213, USA
33 Princeton University, Princeton, NJ 08544, USA
34 INFN-Sezione di Roma and University of Rome, "La Sapienza", I-00185 Rome, Italy
35 Nuclear Physics Institute, St. Petersburg, Russia
36 University of California, San Diego, CA 92093, USA
37 Dept. de Fisica de Particulas Elementales, Univ. de Santiago, E-15706 Santiago de Compostela, Spain
38 Shanghai Institute of Ceramics, SIC, Shanghai, China
39 Bulgarian Academy of Sciences, Institute of Mechatronics, BU-1113 Sofia, Bulgaria
40 Center for High Energy Physics, Korea Advanced Inst. of Sciences and Technology, 305-701 Taejon, Republic of Korea
41 University of Alabama, Tuscaloosa, AL 35486, USA
42 Purdue University, West Lafayette, IN 47907, USA
43 Paul Scherrer Institut, PSI, CH-5232 Villigen, Switzerland
44 DESY-Institut für Hochenergiephysik, O-1615 Zeuthen, FRG
45 Eidgenössische Technische Hochschule, ETH Zürich, CH-8093 Zürich, Switzerland
46 University of Hamburg, W-2000 Hamburg, FRG
47 High Energy Physics Group, Taiwan, China
§ Supported by the German Bundesministerium für Forschung und Technologie
‡ Supported by the Hungarian OTKA fund under contract number 2970.
† Deceased.

References

[1] S.L. Glashow, Nucl. Phys. **22** (1961) 579;
S. Weinberg, Phys. Rev. Lett. **19** (1967) 1264;
A. Salam, Elementary Particle Theory, Ed. N. Svartholm, Stockholm, "Almquist and Wiksell" (1968), 367.

[2] P.W. Higgs, Phys. Lett. **12** (1964) 132, Phys. Rev. Lett. **13** (1964) 508 and Phys. Rev. **145** (1966) 1156;
F. Englert and R. Brout, Phys. Rev. Lett. **13** (1964) 321.

[3] B.L. Ioffe and V.A. Khoze, "What can be expected from experiments on colliding e^+e^- beams with $\approx$ 100 GeV ?", preprint LINP, Leningrad, November 1976;
J.D. Bjorken, Proceedings of the 1976 SLAC Summer Institute on Particle Physics, Stanford, ed. M.C. Zipf (Stanford Linear Accel. Center, Stanford, CA, 1977) p. 1;
J.Finjord, Phys. Scripta **21** (1980) 143.

[4] P.J. Franzini *et al.* in "Z Physics at LEP1", CERN Report CERN-89-08, eds G. Altarelli, R. Kleiss and C. Verzegnassi (CERN, Geneva, 1989) Vol. 2, p. 59 and references therein.

[5] E. Braaten and J.P. Leveille, Phys. Rev. **D22** (1980) 715.

[6] L3 Collaboration, B. Adeva *et al.*, Phys. Lett. **B248** (1990) 203, Phys. Lett. **B252** (1990) 518, Phys. Lett. **B257** (1991) 450;
L3 Collaboration, O. Adriani *et al.*, Phys. Lett. **B294** (1992) 457 and Preprint CERN-PPE/92-163 (1992), to be published in Z Phys. C.

[7] L3 Collaboration, B. Adeva *et al.*, Phys. Lett. **B283** (1992) 454.

[8] ALEPH Collaboration, D.Decamp *et al.*, Phys. Lett. **B236** (1990) 233, Phys. Lett. **B241** (1990) 141, Phys. Lett. **B245** (1990) 289, Phys. Lett. **B246** (1990) 306 and Phys. Rep. **216** (1992) 253.

[9] DELPHI Collaboration, P.Abreu *et al.*, Nucl. Phys. **B342** (1990) 1, Z Phys. **C51** (1991) 25 and Nucl. Phys. **B373** (1992) 3.

[10] OPAL Collaboration, M.Z. Akrawy *et al.*, Phys. Lett. B236 (1990) 224, Z Phys. **C49** (1990) 1, Phys. Lett. **B251** (1990) 211 and Phys. Lett. **B253** (1991) 511;
OPAL Collaboration, P.D. Acton *et al.*, Phys. Lett. **B268** (1991) 122.

[11] L3 Collaboration, B. Adeva *et al.*, Nucl. Instr. and Meth. **A289** (1990) 35.

[12] O. Adriani et al., Nucl. Instr. and Meth. **A302** (1991) 53.

[13] The L3 detector simulation is based on GEANT Version 3.14.
See R. Brun *et al.*, "GEANT 3", CERN DD/EE/84-1 (Revised), September 1987.
The GHEISHA program (H. Fesefeldt, RWTH Aachen Preprint PITHA 85/02 (1985)) is used to simulate hadronic interactions.

[14] T. Sjöstrand and M. Bengtsson, Comput. Phys. Commun. **43** (1987) 367;
T. Sjöstrand in "Z Physics at LEP1", CERN Report CERN-89-08, Vol. 3, p. 143.

[15] E.W.N. Glover, R. Kleiss, J.J. van der Bij, Z Phys. **C47** (1990) 435, J. Hilgart, R. Kleiss and F. Le Diberder Preprint CERN-PPE/92-115 (1992), to be published in Comp. Phys. Communications

[16] M. Consoli and W. Hollik, in "Z Physics at LEP1", CERN Report CERN-89-08, eds G. Altarelli, R. Kleiss and C. Verzegnassi (CERN, Geneva, 1989) Vol. 1, p. 39;
B.A. Kniehl, "Radiative corrections to Higgs production from Z decay", preprint DESY 92–021, February 1992;
F.A. Berends, W.L. van Neerven and G.J.H. Burgers, Nucl. Phys. **B297** (1988) 429.

Tables

Higgs mass (GeV)	30	40	50	55	60	65	70
$H^0\nu\bar{\nu}$ channel	29.5	52.8	57.7	51.8	46.2	28.0	15.0
$H^0e^+e^-$ channel (1991-1992)	58.2	55.2	52.2	50.5	49.4	47.8	44.0
$H^0e^+e^-$ channel (1990)	45.5	38.0	35.0	32.0	29.0	28.0	25.5
$H^0\mu^+\mu^-$ channel	52.6	54.6	53.4	49.0	47.6	41.6	37.0

Table 1: Selection efficiencies (in %) for Higgs events in the different channels. The efficiencies for the $H^0\nu\bar{\nu}$ and $H^0\mu^+\mu^-$ channels are the same for 1990 and 1991–1992 data.

	E (GeV)	θ (*deg.*)	ϕ (*deg.*)
jet_1	58.3 ± 8.9	152.3 ± 2.1	52.9 ± 2.1
jet_2	30.8 ± 5.5	36.6 ± 2.1	284.6 ± 2.1
e^+	4.8 ± 0.1	20.7 ± 0.2	127.7 ± 0.2
e^-	16.2 ± 0.2	63.4 ± 0.1	186.1 ± 0.3

Table 2: The energies (E), the polar angles with respect to the beam line (θ) and the azimuthal angles (ϕ) of the main constituents of the 1992 $H^0e^+e^-$ candidate are indicated. The main parameters of the event are: a visible energy of 109.0 ± 12.5 GeV, a missing mass recoiling against the final state electrons of 67.6 ± 0.7 GeV, an invariant mass of the electron-positron pair of 8.0 ± 0.3 GeV and a measured mass of the hadronic system of 82.2 ± 12.3 GeV.

Figure Captions

Fig. 1 The mass of the dilepton pair $M_{\ell^+\ell^-}$ plotted against the missing mass to the same pair M_{miss} after all other cuts are applied. The remaining candidates together with the expected signal from 30, 40, 50, 60 and 70 GeV Higgs bosons are shown. The line represents the $2M_{\ell^+\ell^-} + M_{miss} > 80$ GeV cut described in the text.

Fig. 2 The 67.6 GeV mass candidate found in 1992 in the $H^0e^+e^-$ channel shown in the plane perpendicular to the beam line. The lines in the TEC represent the reconstructed charged tracks. The size of the symbols indicating individual calorimetric hits (towers in the electromagnetic calorimeter and boxes in the hadron calorimeter) corresponds to the energy deposition of that hit. The towers which appear in the TEC region in this projection belong to the BGO endcaps.

Fig. 3 Number of Higgs events expected in the different channels. The 95% confidence level line is shown and the Higgs mass limit at the 95% C.L. is indicated.

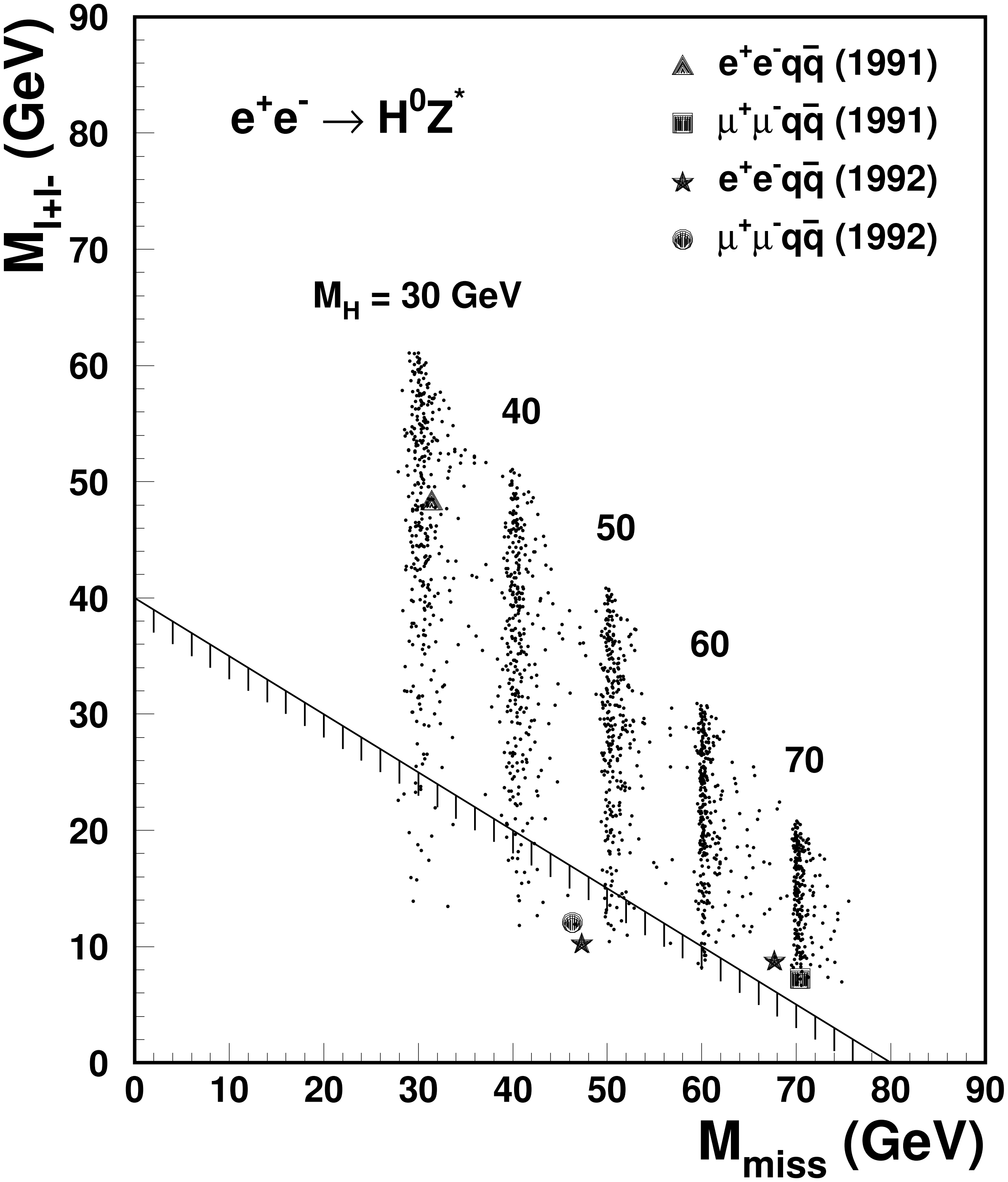
$e^+e^- \rightarrow H^0Z^*$
M_H = 30 GeV
40
50
60
70
$e^+e^-q\bar{q}$ (1991)
$\mu^+\mu^-q\bar{q}$ (1991)
$e^+e^-q\bar{q}$ (1992)
$\mu^+\mu^-q\bar{q}$ (1992)
M_{l+l-} (GeV)
M_{miss} (GeV)
0
10
20
30
40
50
60
70
80
90

Figure 1:

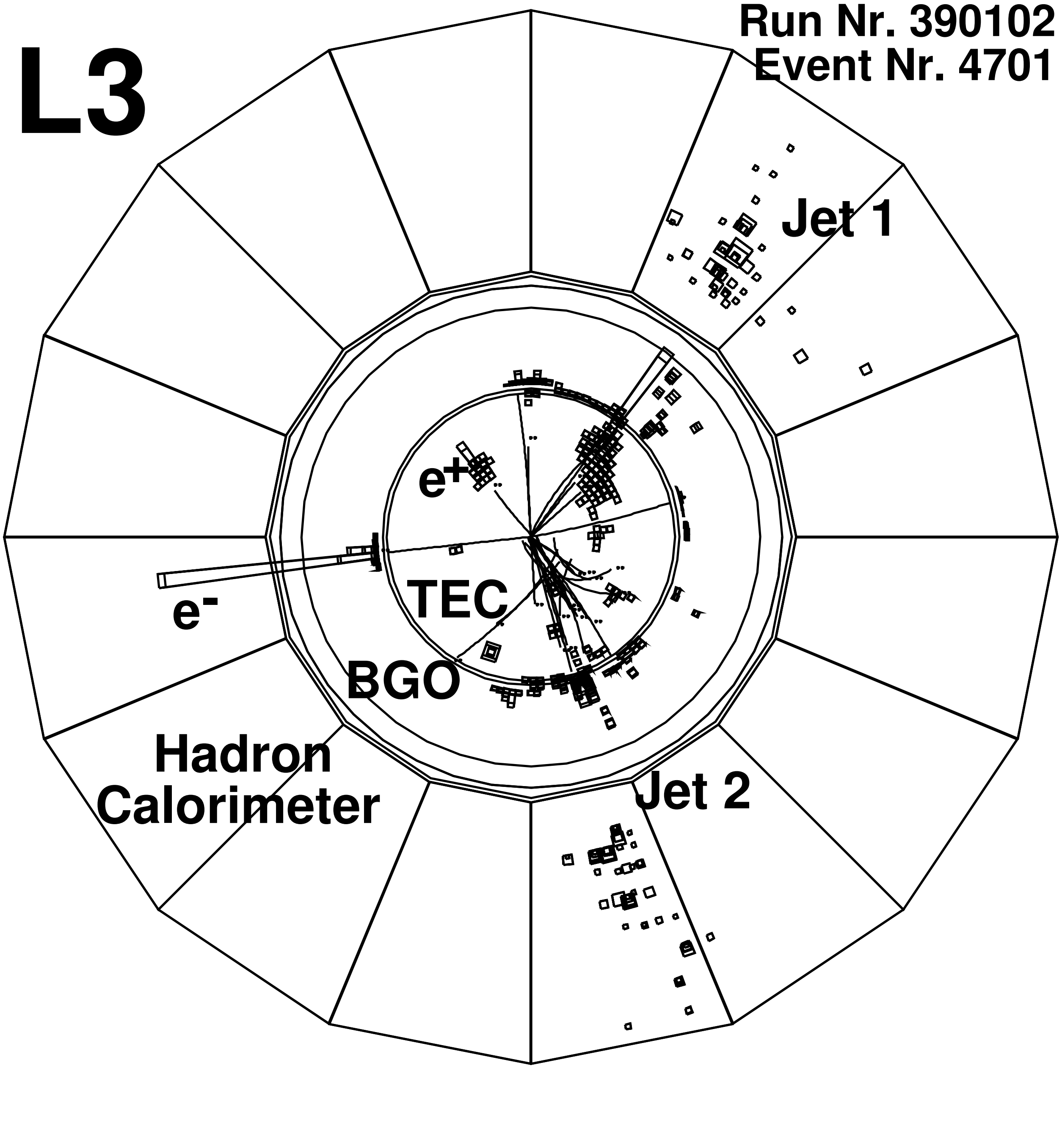
L3
Run Nr. 390102
Event Nr. 4701
Jet 1
e+
TEC
e-
BGO
Hadron
Calorimeter
Jet 2

Figure 2:

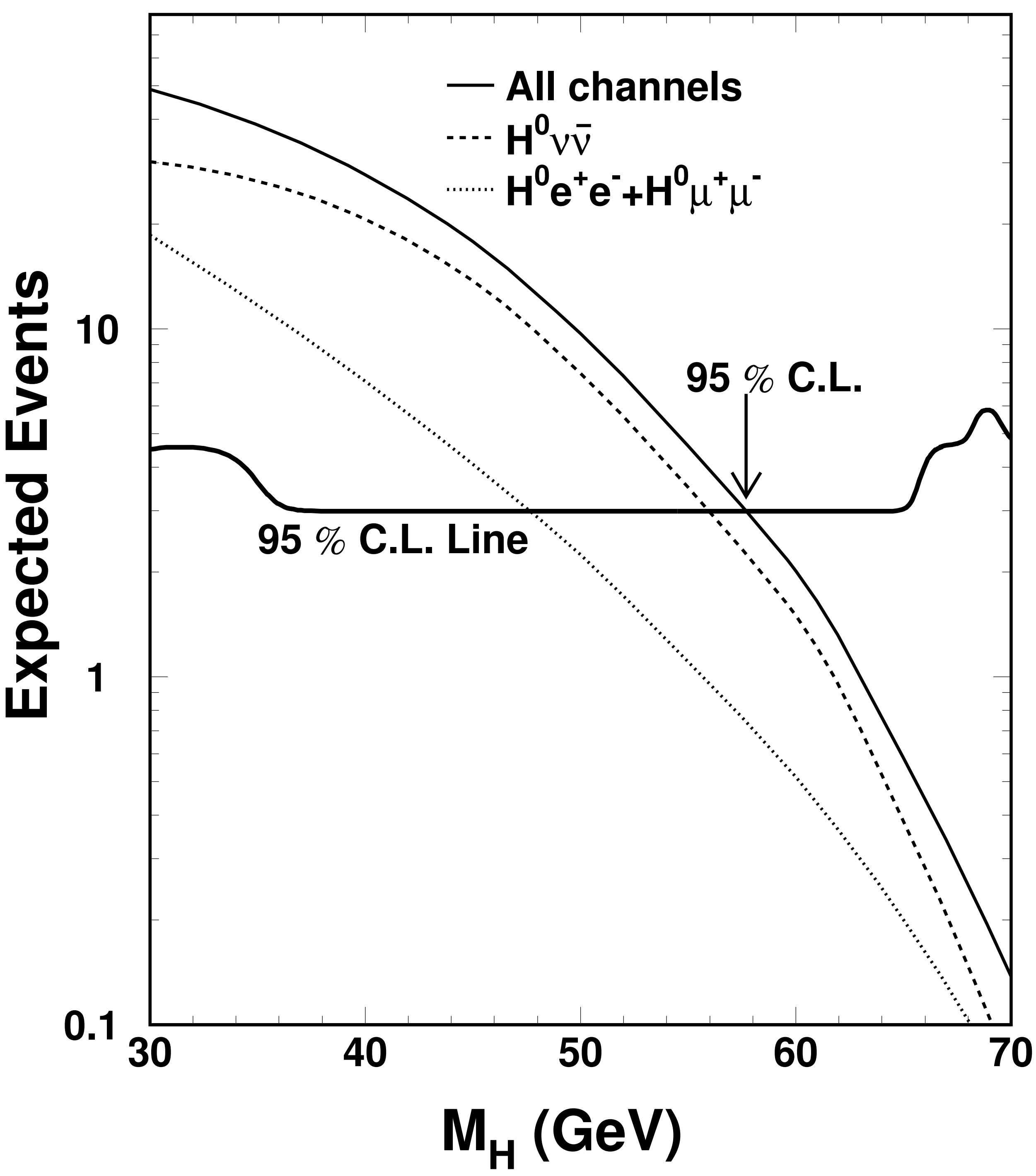
All channels
$H^0\nu\bar{\nu}$
$H^0e^+e^-+H^0\mu^+\mu^-$
95 % C.L.
95 % C.L. Line
Expected Events
10
1
0.1
30
40
50
60
70
M_H (GeV)

Figure 3: